DEVELOPMENT OF A COMPACT LIGHT SOURCE USING A TWO-BEAM-ACCELERATION TECHNIQUE *

P. Piot[1], C. Chen, X. Lu[1], J. G. Power, E. E. Wisniewski,
Argonne National Laboratory, Lemont, IL, USA
C. Jing, S. Kuzikov, Euclid TechLabs, Solon, OH, USA
E. Frame, Northern Illinois University, DeKalb, IL, USA
[1]also at Northern Illinois University, DeKalb, IL, USA

Abstract

The recent demonstration of sub-GV/m accelerating fields at X-band frequencies offers an alternative pathway to designing compact light sources. The high fields were enabled by powering the accelerating structures using short (< 10 ns) X-band RF pulses produced via a two-beam-accelerator (TBA) scheme. In this contribution, we discuss a conceptual roadmap to scale the concept to a ∼ 0.5 GeV accelerator. We present the optimization of a photoinjector and preliminary beam-dynamics modeling of the accelerator. Finally, we discuss ongoing and planned experiments toward developing an integrated proof-of-principle experiment at Argonne National Laboratory employing the a 0.5 GeV TBA-driven accelerator to drive a free-electron laser.

INTRODUCTION

Low-emittance bunches are critical to reducing the footprint of the XFEL: for a given energy the gain length of a single-pass FEL scales with the electron-beam brightness [1]. Consequently, higher brightness translates into shorter undulator lengths. The beam emittance can only degrade between the electron source and the undulator, therefore the source "intrinsic" emittance sets the minimum emittance that can be ultimately attained in the accelerator. A pathway to producing low-emittance bunches is to subject the photocathode to an extremely high electric field as it mitigates the space-charge effect during the emission process and low-energy transport [2]. Currently, most normal-conducting RF guns operate at cathode fields $E_0 \in [80, 140]$ MV/m [3]. Operation at higher fields (∼ 200 MV/m) is currently under investigation using high-frequency [4] or cryogenically-cooled C-band [5] RF guns.

Since 2020, our group has concentrated on the development of an X-band RF (XRF) photoemission gun powered by short (nanosecond) RF pulses and operating at 11.7 GHz; see Fig. 1(a,b) [6, 7] using a two-beam acceleration (TBA) scheme [8]. This operational choice is motivated by the empirical dependence of the breakdown rate (BDR) on the applied surface field E_0 and the RF-pulse duration τ given by BDR $\propto E_0^{30} \tau^5$ [9]. Such a scaling suggests that for a given BDR, reducing the pulse duration significantly enhances the attainable electric field; see Fig. 1(c). The RF

pulse (peak forward power P_{FWD} ∼ 200 MW) was generated by passing a train of 8 high-charge (total charge of Q ∼ 8 × 40 = 320 nC) relativistic (∼ 60 MeV) electron bunches in a power-extraction and transfer structure (PETS) [10]. The high-charge bunches are produced in the Argonne Wakefield Accelerator (AWA) drive-beam accelerator with a time separation of 769 ps corresponding to 1.3 GHz. The developed XRF gun enabled the generation of E-field on the photocathode surface of ∼ 0.4 GV/m with a low BDR and insignificant dark current [7].

The ongoing R&D program leverages this recent accomplishment to focus on forming bright electron bunches and characterizing the associated beam parameters. We are also exploring the building blocks necessary to generate bright ultra-relativistic electron beams for linear collider and light-source applications. This paper summarizes our research program and the latest results.
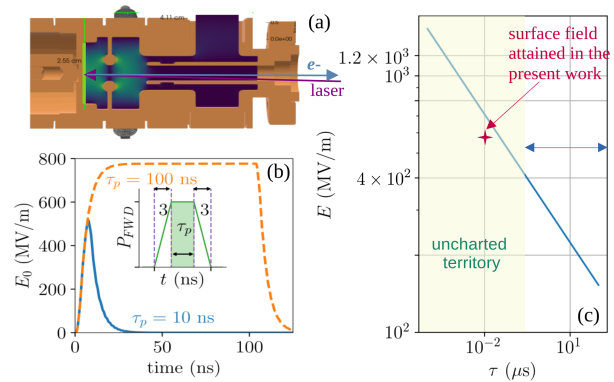

Figure 1: Schematics of the XRF gun with photocathode plane shown in green and electric-field amplitude appearing as a false-color map (a), RF-pulse envelope for short (blue) and (long) RF pulse excitation (b), and example of electric-field scaling with RF pulse duration for a given BDR constant (c). In plot (b), the inset shows the shape of the RF pulse produced from the PETS which yields the blue-trace pulse envelope.

PHOTOEMISSION IN EXTREME FIELDS

Ideally, the beam 4D brightness scales as $B \propto E_0^\nu$ /MTE, the mean transverse energy (MTE) is related to the photocathode physical and chemical properties [2]. The brightness scaling suggests that a low-MTE photocathode combined
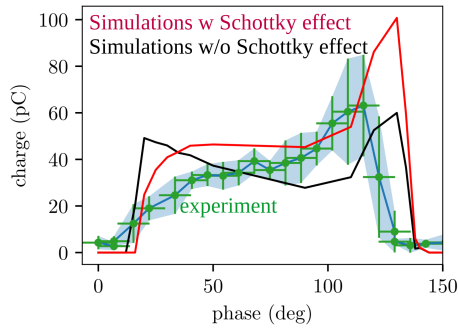
Figure 2: Example of charge emission during a laser-phase scan for $E_0 \simeq 370$ MV/m. The green circles are data points, and the solid traces correspond to numerical simulation with (red trace) and without (black trace) accounting for the Schottky effect.

with a high extraction field offers a path to increasing the brightness. In practice, large fields can affect the MTE due to physical (e.g. cathode surface roughness) or chemical (e.g. position-dependent work function) inhomogeneities [11]. Likewise, the high-field produced in the XRF gun yields a significant charge enhancement due to the effective lowering of the work function (Schottky effect) as illustrated in Fig. 2. Such effects can deteriorate the beam emittance and thus thereby modify the ideal scaling of the brightness with applied E field. A dedicated measurement campaign will investigate the dependence of transverse emittance on the applied field and on the photoemission-laser wavelength in the low-charge limit where space-charge effects are negligible. Such a parametric study will provide insight into the evolution of the MTE in the strong-field regime along with an experimental investigation of the scaling of 4D brightness. In the nominal XRF gun, the copper back plate serves as a photocathode. A future version of the gun will include a load-lock transfer system to facilitate the investigation of other photocathode materials, including low-MTE semiconductor-compound photocathodes.

GENERATION OF 10-MeV EMITTANCE-COMPENSATED BUNCHES

In a second phase, a linac will be installed downstream of the XRF gun to boost the bunch's energy to ~ 10 MeV and for phase-space control. The configuration will ideally recover the intrinsic emittance from the photocathode by implementing the emittance-compensation technique. The results of the beam-dynamics optimization of such a beamline appear in Fig. 3. The beam-dynamics simulations were performed with the program ASTRA and considered a 100-pC bunch. The photocathode-laser temporal shape is taken to be a 3-ps-duration (FWHM) plateau distribution with 300-fs rise time nominally available at AWA. The simulations assume a steady-state regime for the RF as the field variation is negligible over the time it takes for the bunch to transit through the accelerating structures (XRF gun and linac).
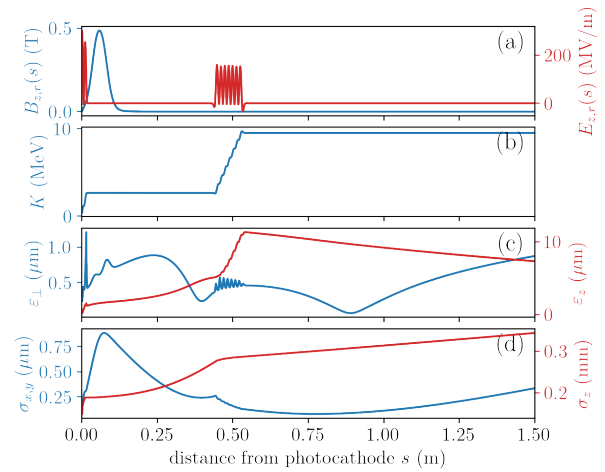

Figure 3: Evolution of beam parameters for a 100-pC beam along the XRF gun+booster beamline. Longitudinal magnetic (blue) and electric (red) fields experienced by the reference particle (a), average kinetic energy (b), rms transverse $\varepsilon_\perp$ and longitudinal ε_z emittances (c) and rms transverse beam sizes $\sigma_{x,y}$ and bunch length σ_z (d).

It should be noted that in practice the short-pulse regime can be employed to power long accelerating structures with each cell powered individually using a distributed-coupling technique [12]. The numerical simulations indicate that a transverse beam emittance of $\varepsilon_\perp \simeq 70$ nm can be attained. However, due to the low final kinetic energy $K \simeq 10$ MeV the emittance is only locally compensated reaching its minimum value at $s \simeq 0.6$ m from the photocathode; see Fig. 3(c). Additionally, the linac can be operated as a buncher to com-
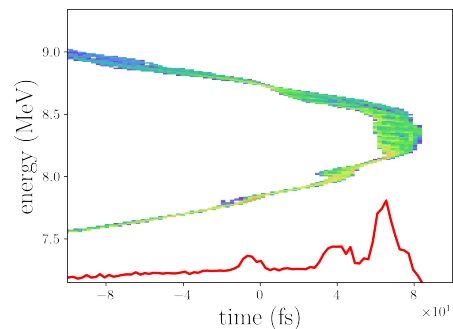

Figure 4: Ballistically bunched longitudinal phase space (false color map) and associated temporal profile (red trace) for a 100-pC bunch downstream of the linac operated off-crest (the head of the bunch is at positive times).

press the longitudinal phase space via ballistic bunching producing a bunch temporal profile with a 20-fs spike; see Fig. 4.

The beam parameters attained with this 10-MeV photoinjector are consistent with requirements associated with the production of ~ 2 keV X-ray source via inverse Compton scattering (ICS) using infrared laser pulses available from the AWA photocathode laser. Likewise, the operating param-

eters of the beamline could also be tuned to support ultrafast electron diffraction experiments. In the near term, we plan to characterize the beam phase spaces downstream of the linac for various operational parameters. Several diagnostics will be developed including a single-shot emittance measurement technique based on a pepper-pot or scanning slits. We will also examine the compression of the bunch via ballistic bunching including the possible use of an X-band deflecting cavity to characterize the longitudinal phase space [13].

PRODUCING 0.5-GeV BRIGHT BEAM

The beam dynamics modeling presented in Fig. 3 was further extended to investigate the required energy to ensure stable emittance compensation without further oscillation. The simulations indicate that accelerating the beam to $K \simeq 50$ MeV is sufficient. The attained beam parameters correspond to a 5D brightness of $B_{5d} \equiv cB/\sigma_z \simeq 3 \times 10^{15}$ A/m^2 comparable to the single-bunch brightness requirements for several next-generation free-electron lasers (FELs) currently under consideration. In order to explore possible FEL configurations based on a TBA scheme that could fit within the AWA facility, a 1-D SASE-FEL model [14] was employed to guide potential working points for SASE-FEL driven by the 0.5-GeV electron beam. In our calculations, the FEL-saturation length was restricted to 5-m (due to real-estate constraints at AWA) and we considered an undulator with period $\lambda_u = 23$ mm and undulator parameter $K = 2.5$ yielding a resonant wavelength $\lambda \simeq 50$ nm; see Fig. 5.
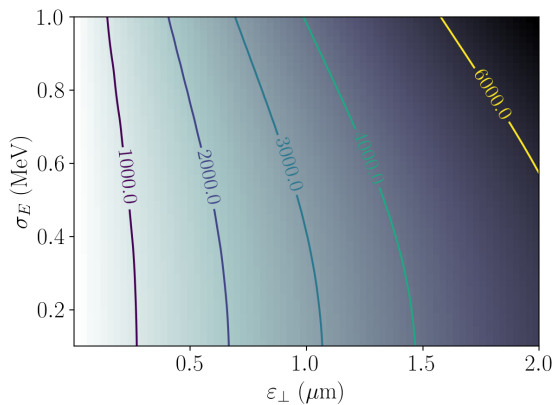
Figure 5: Required peak current (isoclines with labels in Ampère) as a function of transverse emittance $\varepsilon_\perp$ and energy spread σ_E. The saturation length is set to 5 m and the SASE FEL radiation wavelength is $\lambda = 45.9$ nm.

Given the simulated performances of the injector ($\varepsilon_\perp \leq$ 100 nm), and accounting for emittance dilution during acceleration and manipulation prior to the undulator, a general accelerator architecture coupling the photoinjector to a high-energy linac was formulated. In its current implementation, we anticipate the photoinjector after further acceleration to 140 MeV would be coupled to a K-band linac operating at 26 GHz (20th harmonic of 1.3 GHz). Preliminary 1D-1V nu-

merical simulations of the longitudinal beam dynamics [15] associated with the generation of a low-emittance bunch and its acceleration to a final energy of 0.5 GeV appear in Fig. 6.
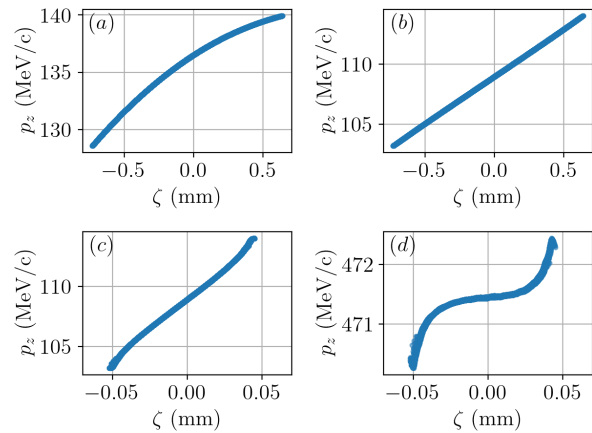
Figure 6: Evolution of the longitudinal phase space (ζ, p_z) along the X and K-band linacs. The snapshots give the distribution at the injector exit simulated from ASTRA after acceleration in the X-band linac (a), downstream of a 26-GHz linac for phase-space linearization (b), after a bunch-compression beamline (c) and after further acceleration in a 26-GHz linac to the final energy (d).

SUMMARY & OUTLOOK

Preliminary experimental tests on a TBA concept have produced high surface fields that could support the compact generation and acceleration of bright electron bunches. The design of such a compact accelerator to produce 0.5-GeV bunches is under investigation at the AWA facility. Preliminary estimates indicate the contemplated beam brightness could support the lasing of a SAFE-FEL at 50 nm using a 5-m undulator. Further numerical simulations of the beam dynamics including collective effects are underway to further optimize the accelerator design.

ACKNOWLEDGMENTS

REFERENCES

[1] S. Di Mitri, "On the importance of electron beam brightness in high gain free electron lasers," *Photonics*, vol. 2, no. 2, pp. 317–341, 2015. doi:10.3390/photonics2020317

[2] D. Filippetto, P. Musumeci, M. Zolotorev, and G. Stupakov, "Maximum current density and beam brightness achievable by laser-driven electron sources," *Phys. Rev. Spec. Top. Accel Beams*, vol. 17, p. 024 201, 2 2014.
doi:10.1103/PhysRevSTAB.17.024201

[3] Y. Ding *et al.*, "Measurements and simulations of ultralow emittance and ultrashort electron beams in the linac coherent light source," *Phys. Rev. Lett.*, vol. 102, p. 254 801, 25 2009.
doi:10.1103/PhysRevLett.102.254801

[4] R. A. Marsh, G. G. Anderson, S. G. Anderson, D. J. Gibson, C. P. J. Barty, and Y. Hwang, "Performance of a second generation X-band RF photoinjector," *Phys. Rev. Accel. Beams*, vol. 21, p. 073 401, 7 2018.
doi:10.1103/PhysRevAccelBeams.21.073401

[5] R. R. Robles, O. Camacho, A. Fukasawa, N. Majernik, and J. B. Rosenzweig, "Versatile, high brightness, cryogenic photoinjector electron source," *Phys. Rev. Accel. Beams*, vol. 24, p. 063 401, 6 2021.
doi:10.1103/PhysRevAccelBeams.24.063401

[6] S. Kuzikov *et al.*, "An X-Band Ultra-High Gradient Photoinjector," in *12th International Particle Accelerator Conference*, 2021.
doi:10.18429/JACoW-IPAC2021-WEPAB163

[7] W. H. Tan *et al.*, "Demonstration of sub-GV/m accelerating field in a photoemission electron gun powered by nanosecond *X*-band radio-frequency pulses," *Phys. Rev. Accel. Beams*, vol. 25, p. 083 402, 8 2022.
doi:10.1103/PhysRevAccelBeams.25.083402

[8] R. Corsini, "Final Results From the Clic Test Facility (CTF3)," in *Proc. of International Particle Accelerator Conference (IPAC'17), Copenhagen, Denmark, 14-19 May, 2017*, Copenhagen, Denmark, 2017, pp. 1269–1274.
doi:10.18429/JACoW-IPAC2017-TUZB1

[9] A. Grudiev, S. Calatroni, and W. Wuensch, "New local field quantity describing the high gradient limit of accelerating structures," *Phys. Rev. Spec. Top. Accel Beams*, vol. 12, p. 102 001, 10 2009.
doi:10.1103/PhysRevSTAB.12.102001

[10] M. Peng *et al.*, "Generation of High Power Short Rf Pulses using an X-Band Metallic Power Extractor Driven by High Charge Multi-Bunch Train," in *10th International Particle Accelerator Conference*, 2019, MOPRB069.
doi:10.18429/JACoW-IPAC2019-MOPRB069

[11] G. S. Gevorkyan, S. Karkare, S. Emamian, I. V. Bazarov, and H. A. Padmore, "Effects of physical and chemical surface roughness on the brightness of electron beams from photocathodes," *Phys. Rev. Accel. Beams*, vol. 21, p. 093 401, 9 2018. doi:10.1103/PhysRevAccelBeams.21.093401

[12] S. Tantawi, M. Nasr, Z. Li, C. Limborg, and P. Borchard, "Design and demonstration of a distributed-coupling linear accelerator structure," *Phys. Rev. Accel. Beams*, vol. 23, p. 092 001, 9 2020.
doi:10.1103/PhysRevAccelBeams.23.092001

[13] S. Kim *et al.*, "Longitudinal Bunch Shaping Using an X-Band Transverse Deflecting Cavity Powered by Wakefield Power Extractor at Argonne Wakefield Accelerator Facility," in *Proc. 13th International Particle Accelerator Conference (IPAC'22)*, Bangkok, Thailand, 2022, paper WEOZSP1, pp. 1655–1658.
doi:10.18429/JACoW-IPAC2022-WEOZSP1

[14] M. Xie, "Design optimization for an x-ray free electron laser driven by slac linac," in *Proceedings Particle Accelerator Conference*, vol. 1, 1995, 183–185 vol.1.
doi:10.1109/PAC.1995.504603

[15] W. H. Tan, P. Piot, and A. Zholents, "Formation of temporally shaped electron bunches for beam-driven collinear wakefield accelerators," *Phys. Rev. Accel. Beams*, vol. 24, p. 051 303, 5 2021.
doi:10.1103/PhysRevAccelBeams.24.051303